THE ASTROPHYSICAL JOURNAL SUPPLEMENT SERIES, 127:267–273, 2000 April


# EQUATION OF STATE AND MATERIAL PROPERTY MEASUREMENTS OF HYDROGEN ISOTOPES AT THE HIGH-PRESSURE, HIGH-TEMPERATURE, INSULATOR-METAL TRANSITION

R. CAUBLE, P. M. CELLIERS, G. W. COLLINS, L. B. DA SILVA, D. M. GOLD, M. E. FOORD, K. S. BUDIL, AND R. J. WALLACE
Lawrence Livermore National Laboratory, P.O. Box 808, Livermore, CA 94550; cauble@jllnl.gov

AND

A. NG
University of British Columbia, Vancouver, BC, Canada; nga@physics.ubc.ca
*Received 1999 January 19; accepted 1999 July 8*

## ABSTRACT

A high-intensity laser was used to shock compress liquid deuterium to pressures between 0.22 and 3.4 megabars (Mbar). Shock density, pressure, and temperature were determined using a variety of experimental techniques and diagnostics. This pressure regime spans the transformation of deuterium from an insulating molecular fluid to an atomic metallic fluid. Data reveal a significant increase in compressibility and a temperature inflection near 1 Mbar, both indicative of such a transition. Single-wavelength reflectivity measurements of the shock front demonstrated that deuterium shocked above $\sim 0.5$ Mbar is indeed metallic.

*Subject headings:* atomic processes — equation of state — methods: laboratory — shock waves

## 1. INTRODUCTION

Hydrogen at high pressure is one of the most difficult to understand. Having only a single electron, it shows characteristics of both alkalis and halogens (Ashcroft 1995; Hemley & Ashcroft 1998). At low pressure, hydrogen isotopes are halogenous, covalent diatomic molecules that form insulators. With increasing pressure, the isotopes transform into alkali metals although the mechanism is complex and unknown. The metallic transition and its effects on the equation of state (EOS) at pressures near 1 megabar (Mbar) are integral to models of many hydrogen-bearing astrophysical objects (Van Horn 1991), including giant planets (Smoluchowski 1967; Hubbard 1981; Chabrier et al. 1992), brown dwarfs (Saumon et al. 1992; Hubbard et al. 1997), and low-mass stars (Chabrier & Baraffe 1997).

Figure 1 shows the phase space of hydrogen in the vicinity of the finite-temperature insulator-metal transition in the regime of the fluid metal-insulator phase transition (Saumon, Chabrier, & Van Horn 1995). Here $\Gamma = e^2(4\pi/3n)^{1/3}/kT$, where $n$ is the particle density, is a measure of the interparticle correlation strength; a value of $\Gamma > 1$ signifies strong coupling between the fluid constituents and a commensurate lack of simplifying assumptions that enable theoretical calculations. The Fermi energy is $\varepsilon_F$; for temperatures $kT < \varepsilon_F$, matter is partially degenerate.

This regime of high density and extreme pressure is fundamentally difficult to address theoretically: it is a dynamic, strongly correlated, partially degenerate composite of $H_2$, H, $H^+$, and electrons, as well as molecular chains, where no simple approximation is available. It is a high-pressure regime where both molecular dissociation and ionization can be initiated through density as well as thermal effects. Early EOS models either did not include these effects or predicted that their consequences for the EOS would be small (Kerley 1972, 1980; Ross, Ree, & Young 1983). More recent models and simulations vary in their predictions. Indeed, theories disagree about the nature of the phase boundary: it is not known whether the phase transition is continuous or abrupt. Recent molecular dynamics simulations largely replicate the earlier models (Lenosky, Kress, & Collins 1997). Ross (1998) predicts significant modifications to the EOS through a continuous dissociative transition, while other models (Saumon & Chabrier 1989; Reinholz, Redmer, & Nagel 1995) and computer simulations (Magro et al. 1996; Militzer, Magro, & Ceperley 1998) predict a first-order phase transition from the molecular to the metallic phase. It is a regime where data are needed to guide theory. However, until recently, the regime of the metal-insulator transition was experimentally unattainable.

Most theories predict less than 3 Mbar for the insulator-metal transition pressure along the 0 K isotherm (Wigner & Huntington 1935; Natoli, Martin, & Ceperley 1993). Static (diamond anvil cell) experiments (Loubeyre et al. 1996; Hemley et al. 1996) at these pressures have not shown evidence of metallization (Narayana et al. 1998). However, dynamic (shock) experiments have yielded evidence of changes associated with an increase in the number of charge carriers at pressures much lower than 3 Mbar. An increase of 3 orders of magnitude in the electrical conductivity of fluid hydrogen was observed after the fluid was multiply shocked to 1.4 Mbar at a temperature of 3000 K where the isotope is in a molecular fluid phase (Weir, Mitchell, & Nellis 1996). Discussed below are results of measurements of the EOS of strongly shocked deuterium where the transition from an insulating state to the metallic phase has been observed. (EOSs for all hydrogen isotopes are identical except for a scale factor in density. Deuterium was used because, for a given shock intensity, higher pressures can be reached in [higher density] deuterium than in hydrogen.)

Shocks impart entropy to the sample so that the sample does not follow an isentrope but rather a Hugoniot; so dynamic experiments access a different part of the EOS than static measurements. The Hugoniot is the locus of density, pressure, and energy states in a material following passage of a single shock and is a well-defined curve on the EOS surface (see Fig. 1).

Shock wave experiments using light gas guns have produced Hugoniot data on deuterium (initial density $\rho_0 = 0.17$ g cm$^{-3}$) up to 0.23 Mbar ($\rho = 0.58$ g cm$^{-3}$ and

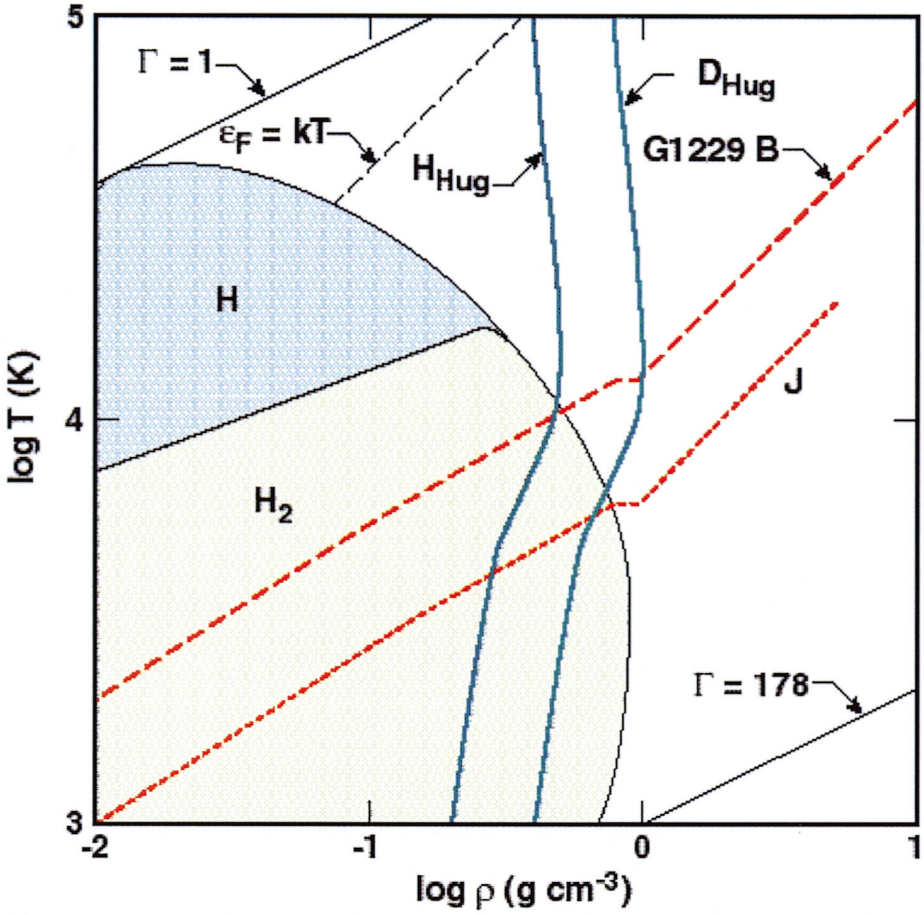


FIG. 1.—Model phase diagram of hydrogen in the regime of the fluid metal-insulator phase transition (Saumon, Chabrier, & Van Horn 1995). "$H_2$" and "H" are regions that are mainly molecular and atomic hydrogen, respectively; outside of these regions hydrogen is primarily an ionized fluid. "J" is a model isentrope for Jupiter (Saumon et al. 1995); "G1229 B" is an isentrope for brown dwarf G1229 B (Hubbard et al. 1997). "$H_{Hug}$" and "$D_{Hug}$" are model hydrogen and deuterium Hugoniots (Ross 1998).

$T = 3900$ K), below the metal-insulator transition (Nellis et al. 1983; Holmes, Ross, & Nellis 1995). Temperature measurements of shocked deuterium (Holmes et al. 1995; Nellis, Ross & Holmes 1995) first indicated that the hydrogen EOS may be softer (more compressible) than had been earlier believed. Gas guns in use at present are not capable of producing pressures on the deuterium Hugoniot above about 0.25 Mbar. High-power lasers have long been known capable of driving higher pressure shocks but accurate, near-Mbar absolute EOS data had never been obtained using lasers.

## 2. MEASURING EOS DATA WITH LASERS

The use of intense lasers to drive strong shocks in matter with the purpose of establishing measurable high pressure states has long been considered (van Kessel & Sigel 1974; Ng, Parfeniuk, & Da Silva 1985; Löwer et al. 1994; Koenig et al. 1995; Evans et al. 1996). However, several obstacles have to be overcome to obtain reliable data.

First, the shock produced must be spatially uniform. A modulated shock possesses a range of pressure and densities along the shock front and is unsuitable for measurements. This issue can be partially addressed by target design and smoothing of the beam. The shock should also be planar. Producing a strong shock with a high laser intensity obtained by focusing to a small spot may succeed only in driving a near-spherical shock wave into the target, making experimental interpretation difficult. A laser spot that is too small will also be subject to edge effects, that is, rarefaction waves releasing from the perimeter of the spot and moving radially inward. If the spot diameter is small, these rarefactions can reach the center of the spot on the timescale of the measurements, compromising the results. Second, the shock should be steady in time and long in duration. This allows measurements over longer times with enhanced precision. These two points specify that high laser intensity is necessary for high-pressure shock production but it is not sufficient. High laser *energy* provides the capability of producing spatially large shocks at high pressures and driving them uniformly over long periods. In practice, for laser experiments, a large spatial scale is about 1 mm and long times are 10 ns. This puts a burden on diagnostic capabilities, but the national inertial confinement fusion program has pushed the development of such instrumentation for high power lasers.

The last difficulty associated with laser-driven EOS measurements is so-called preheat; that is, heating of the sample prior to the intended shock arriving in the sample. A single shock drives a sample to a point on the Hugoniot where conservation relations require that two independent parameters be measured to obtain an absolute EOS data point. The shock speed, $U_s$, particle (or pusher) speed $U_p$, final

pressure $P$, and final density $\rho$ are related by

$$P - P_0 = \rho_0 U_s U_p \quad (1)$$

and

$$\rho/\rho_0 = U_s/(U_s - U_p)\,, \quad (2)$$

where $\rho_0$ is the initial density, $P_0$ is the initial pressure, and $\rho/\rho_0$ is the compression (Zeldovich & Raizer 1966). The experiments measure of $U_s$ and $U_p$. By equation (2), only the compression is determined in a shock experiment, not the final density, so that $\rho$, must be known in order to obtain $\rho$. If the sample is disturbed prior to shock arrival, $\rho_0$ can be reduced by volume expansion if the sample is heated or increased by a preshock or thermal expansion of other parts of the target. In either case, both $P_0$ and $\rho_0$ will be unknown and the determination of the final state will be in error. In the experiments described below, samples of liquid deuterium at 20 K were located less than 200 $\mu$m from a $20 \times 10^6$ K laser-matter plasma, so the results depended on knowing that the deuterium was not affected by the nearby heat source.

## 3. EOS MEASUREMENTS OF DEUTERIUM FROM 0.25 TO 3.4 Mbar

The high-energy Nova laser (Campbell 1991) was used to shock liquid deuterium to pressures that span the metal-insulator transition on the Hugoniot. Measurements of $U_s$ and $U_p$ were made that, via equations (1) and (2), yielded final pressure and density. In addition, the shock temperature was measured up to 2.4 Mbar on the Hugoniot. Last, a reflective diagnostic provided confirmation that the experiments spanned the metal-insulator phase boundary.

Liquid deuterium at 20 K was contained in a 1.5 or 1 mm diameter, 0.45 mm long cylindrical cell machined into a copper block. One end of the cell was sealed with a metal (Al or Ce) disk that acted as a shock pusher; the outside of each pusher was coated with a low atomic number ablator. X-ray–transmitting windows of Be foils allowed radiography transverse to the shock direction through the sides of the cell. The sample could also be viewed with several instruments from behind through a 0.5 mm thick sapphire window. A spatially smoothed Nova laser beam ($\lambda_L = 527$ nm) with an intensity of $10^{13}$ to $3 \times 10^{14}$ W cm$^{-2}$ irradiated the ablator for 5 to 10 ns. The ablator minimized production of high energy X-rays in the laser plasma and drove a shock into the metal pusher. When the shock reached the rear of the pusher, the pusher/deuterium interface released into the deuterium at the speed $U_p$, while the shock propagated ahead at the speed $U_s$. The radiography source was a Nova laser–heated Fe foil (see Fig. 2).

### 3.1. *Pressure and Density on the Hugoniot*

Using transverse radiography, the positions of the shock front and the interface were tracked as a function of time to obtain measurements of $U_s$ and $U_p$ for each experiment. A streak radiograph is shown in Figure 3. The pusher is opaque to backlighter X-rays so the interface is the boundary between the light and dark regions. At $t = 0$, the shock crosses the interface and the interface surface begins to move; by 3 ns, the interface is moving at the final speed $U_p$. The shock front is visible as a dark line propagating ahead of the interface since backlighter X-rays grazing the shock front are refracted out of the collection optics. The slope of this line is $U_s$.

The sapphire window at the back of the cell admitted a probe laser. On some experiments a Michelson interferometer was used to image the rear of the pusher through the unshocked deuterium. The interferometer monitored the surface position for evidence of radiative heating of the target (Da Silva et al. 1997). The demonstrated lack of

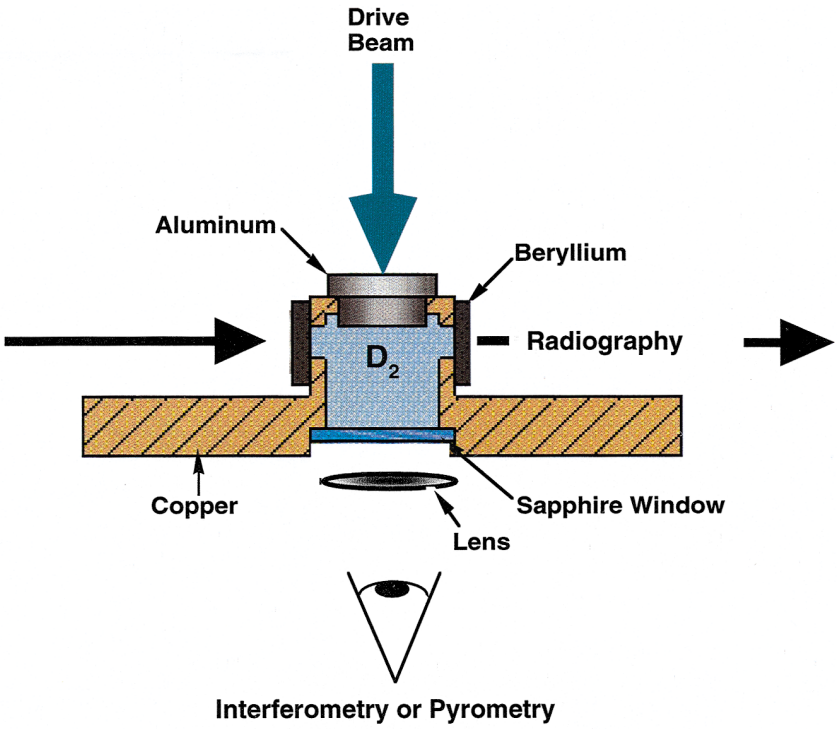


FIG. 2.—Diagram of the cryogenic cell to measure properties of the EOS of deuterium

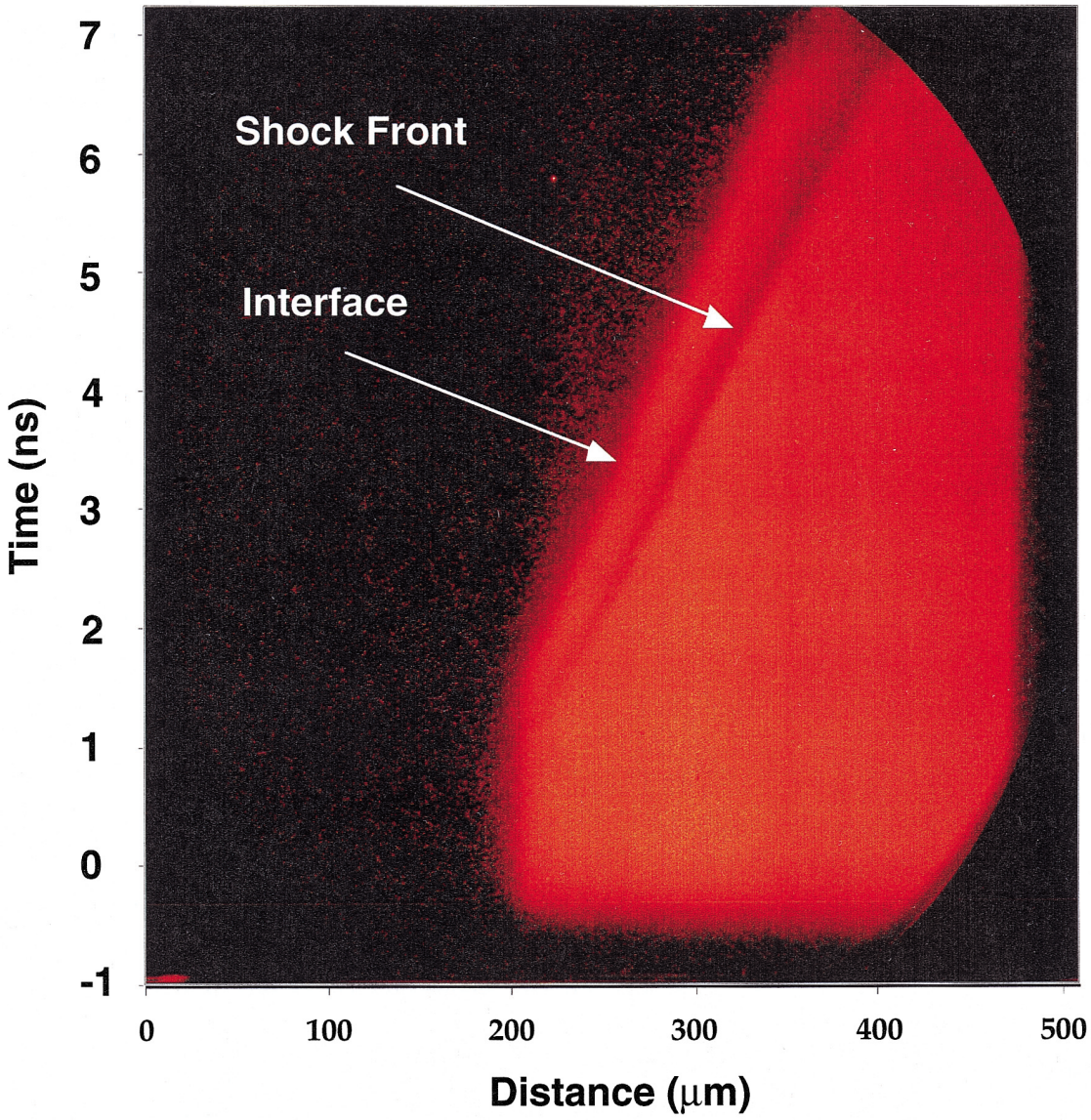


FIG. 3.—Transverse streak transmission radiograph of a deuterium EOS target with a Be pusher at a laser intensity of $7.6 \times 10^{13}$ W cm$^{-2}$. Shock release into the deuterium is at $t = 0$. The image shows a shock decelerating until $t = 3$ ns where it becomes steady where the slopes of the interface and shock are $U_p$ and $U_s$, respectively.

sample preheat allowed us to confidently use laser-driven shocks for EOS measurements on deuterium (Gupta & Sharma 1997).

Pressure-density data are shown in Figure 4 (Collins et al. 1998a). At the lowest compression, the laser data agree with gas gun results. However, there is a pronounced compressibility above 0.3 Mbar, turning around at about 1 Mbar. At 1 Mbar, the model used in the SESAME EOS tables (Kerley 1972), as well as the Ross et al. (1983) model (not shown but similar to SESAME) show the deuterium Hugoniot density is 0.68 g cm$^{-3}$ ($\rho/\rho_0 = 4$), whereas the data show a density of 1.0 g cm$^{-3}$ ($\rho/\rho_0 = 5.88$), an increase of $\sim 50\%$. This softer EOS is similar to the models of Saumon & Chabrier (1991, 1992) and Ross (1998). These models use minimization of the free energy of a mixture of molecular, atomic, and ionic species to determine species concentrations and establish thermodynamics of the mixture. The methods, and in particular the interspecies potentials, are different in each case. Ross also uses the expedient of a term determined by gas gun shock data. The Monte Carlo simulations (Militzer et al. 1998) are the closest to an unmodeled theory. They represent numerical integration of the interactions of a finite set of individual nuclei and electrons. They show a high compression but at a lower pressure than the data evince. The high-temperature ACTEX model (Rogers 1986; Rogers, Swenson, & Iglesias 1996) also predicts a high shock density. However, at higher pressure these latter models lie to the low-density site of the data. A molecular dynamics simulation Hugoniot (Lenosky et al. 1997) predicts only slight effects of dissociation and ionization on the Hugoniot.

### 3.2. *Temperature on the Hugoniot*

Temperature is fundamental to thermodynamics and EOS models, but it is not part of the Hugoniot relations that allow experimental determination of pressure, density, and internal energy of a shock-compressed state. Temperature measurements provide important and independent detail of the state of the system. It was the gas gun shock

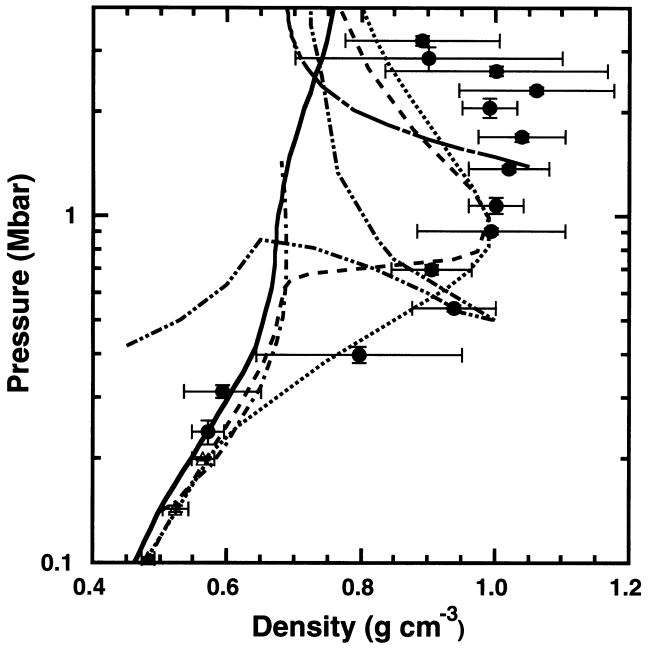


FIG. 4.—Hugoniot data presented as pressure vs. density. Gas gun data (*triangles*) are shown (Nellis et al. 1983; Holmes, Ross, & Nellis 1995). The EOS model of Ross (1998) is shown as the dotted line. Other theoretical Hugoniots are from the widely used SESAME tabular EOS: Kerley (1972, 1980; *solid line*), the hydrogen EOS of Saumon & Chabrier (1991, 1992; *dashed line*), ACTEX theory (Rogers 1986; *long dash-dotted line*), path integral quantum Monte Carlo simulations (Militzer et al. 1998; *chain double dotted line*), and tight binding molecular dynamics simulations (Lenosky et al. 1997; *dot-dashed line*).

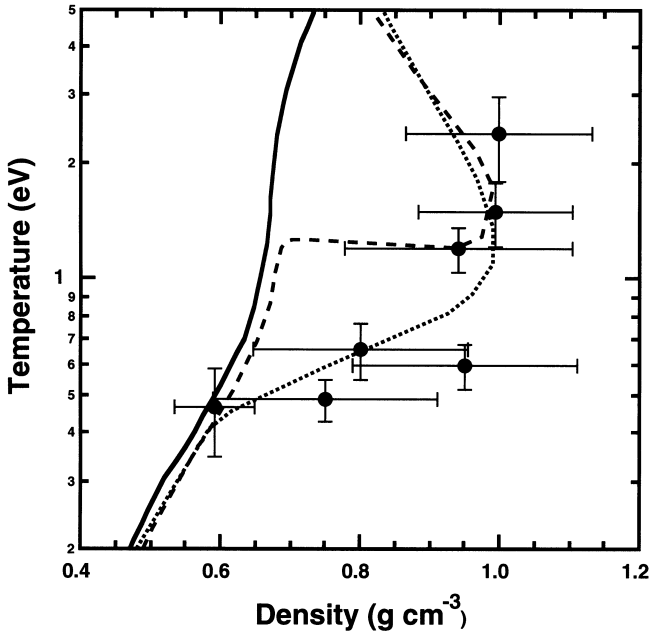


FIG. 5.—Hugoniot temperatures determined from pyrometry of the shock front of laser-shocked deuterium. Curves are the same as Figure 4.

temperature measurements of Holmes et al. (1995) on double-shocked deuterium that first indicated that there might be a softening of the EOS in the Mbar regime. They constructed an EOS model that spanned the transition from an insulating state to a dissociated metallic state using a mixing model (Ross 1998). This provided a quantitative prediction of the transition from the molecular fluid into the atomic metal phase along the (single-shock) Hugoniot. The resulting model Hugoniot exhibited significant softening at pressures above 0.25 Mbar, a prediction that was then confirmed by laser-produced shock experiments (Da Silva et al. 1997; Collins et al. 1998).

Temperature determinations were made for Mbar-shocked deuterium using multifrequency pyrometry, similar to the experiments of Holmes et al. (1995). Emission from the shock front was observed through the sapphire window in the rear of the cell. Measurements of the absolute spectral radiance $I(\lambda)$ of the shock front at several wavelengths were made using a fiber-coupled multichannel pyrometer. The temperature was found by fitting $I(\lambda)$ to a graybody Planck spectrum,

$$I(\lambda) = \varepsilon \frac{2\pi hc^2}{\lambda^5} \left( \exp \frac{hc}{\lambda k_b T} - 1 \right)^{-1}, \quad (3)$$

where the emissivity $\varepsilon$ and temperature $T$ were fitting coefficients. Details can be found in Collins et al. (2000). Selected results of these measurements are shown in Figure 5 where the density was determined by transverse radiography simultaneous with the end-on pyrometry. The data appear to show an inflection as the Hugoniot pressure enters the regime of high compressibility (see Fig. 4). The Saumon-Chabrier model has an evident inflection (evidence of their predicted first-order phase transition), but the temperature is too high. The Ross mixing model predicts Hugoniot temperatures that are similar to the data but without an evident inflection (evidence of that model's assumption of a continuous phase transition). As with the pressure-density data, there is no evidence for any abrupt phase behavior on the Hugoniot. The SESAME model, which shows little effect of the phase transition on the EOS predicts a temperature that rapidly rises along the Hugoniot.

### 3.3. *Metallization of Deuterium on the Hugoniot*

High-pressure laser-driven data presented in the two previous sections showed that something significant occurs on the Hugoniot of hydrogen isotopes near 1 Mbar pressure. The compressibility increases dramatically beginning at about 0.3 Mbar, increases further up to about 1 Mbar, then turns around at higher pressures (see Fig. 4). At the same time the temperature remains low at low pressures compared to early models and increases significantly only after the turnaround (see Fig. 5). In order to investigate the material properties in this regime, a reflecting diagnostic called a velocity interferometer (Barker & Hollenbach 1972; Celliers et al. 1998) was positioned to view the shock front from the rear of the cell through the sapphire window. Velocity interferometry measures the Doppler shift of light reflected from a moving surface, in this case of a probe laser with wavelength = 1064 nm. The recorded fringe shift is directly proportional to the Doppler shift and, therefore, to the velocity of the reflecting surface. In Figure 6, before shock breakout at $t = 0$, the reflected light originates from the motionless pusher surface and the fringes are stationary. For $t > 0$, the pattern shifts to a new phase since the reflecting surface is no longer the pusher surface but the shock front moving at $U_s$ in the deuterium sample. Velocity interferograms produced shock speeds that equal those

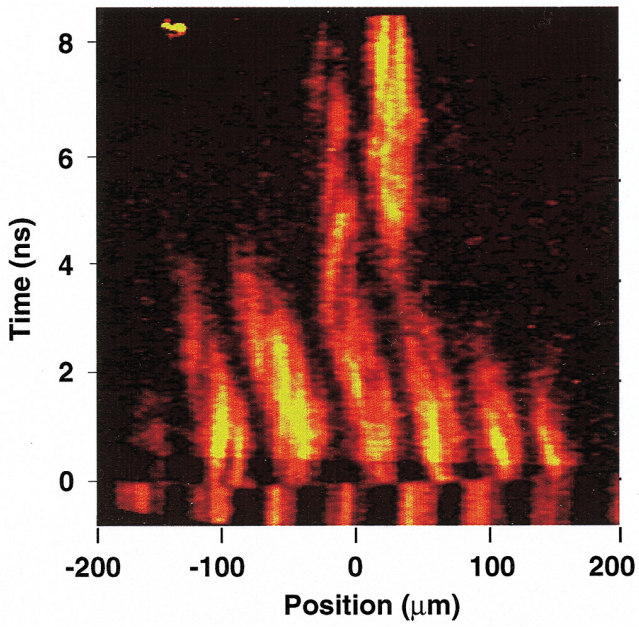


FIG. 6.—End-on streak velocity interferogram of the shock front in the same target as shown in Fig. 3. Deceleration of the shock is evinced as fringe motion from $t = 0$ to $t = 3$ ns, then the shock becomes steady. The high reflectivity from the shock front indicates a metallic state.

determined from radiography but with greater accuracy. In addition to the EOS experiments that were designed to produce a single-shock pressure along with a constant shock speed, additional experiments were performed with an attenuating shock pressure and consequent decelerating shock speed. The purpose of these latter shots was to measure reflectivity over a broad range of shock speed; the shock speed could be turned into pressure from our EOS data. Figure 6 is an interferogram of one of the attenuating shocks.

The interferometer supplied instantaneous measurements of the (single-wavelength) reflectivity of the shock front. At low shock pressures, the reflectivity is a few percent. However, above 0.5 Mbar the measured reflectivities are around 60%, characteristic of a metal (Celliers et al. 2000). Since the temperature of the shocked deuterium is $\sim 7500$ K, much less than the ionization potential, the high reflectivity is due to free electrons produced by a combination of density and thermal effects. In plasma physics, this is referred to as pressure ionization. The temperature is also much less than the Fermi energy $\varepsilon_F$ ($\sim 150{,}000$ K) so the term metal is appropriate.

## 4. CONCLUSIONS

A high-power laser has been used to access regimes of pressure, density, and temperature of hydrogen isotopes that have been unexplored until now. In order to reach these conditions and return usable results, a number of experimental techniques were developed and employed.

The data show that deuterium is a near-fully dissociated, partially ionized metallic fluid, at pressures between 0.5 and 0.8 Mbar and temperatures of around 6–10,000 K. The process begins at about 0.3 Mbar on the Hugoniot and continues until at least 1 Mbar. Some of the higher pressure data lie to the high-compression side of all of the theoretical Hugoniots; these data are not yet explained, but there is a trend in the data toward the high pressure ideal gas compression limit of 4.

The data offer an assessment of the EOS of hydrogen isotopes on both sides of the metal-insulator phase transition. The hydrogen compressibility undergoes a significant increase and the temperature is 0.07–0.3 that of the Fermi temperature where the measured reflectivity indicates that deuterium is transitioning from a molecular insulating state to a metallic one. The data indicate that there is no first-order phase transition on the Hugoniot (this does not preclude the existence of a first-order phase boundary elsewhere in the EOS phase space).

These data were obtained in conditions that are not very different from those found in the atmospheres of giant planets and outer envelopes of low-mass stars that are largely hydrogen. The measured Hugoniot and confirmation of the existence of a metallic state at relatively low pressures will constrain theoretical models of the equations of state of hydrogen isotopes.

The authors would like to thank G. Chabrier, N. C. Holmes, W. J. Nellis, M. Ross, F. J. Rogers, D Saumon, and D. A. Young for highly informative by Lawrence Livermore National Laboratory under contract no. W-7405-Eng-48.

## REFERENCES

Ashcroft, N. W. 1995, Phys. World, 8 (July), 43
Barker, L. M., & Hollenbach, R. E. 1972, J. Appl. Phys., 43, 4669
Campbell, E. M. 1991, Laser Part. Beams, 9, 209
Celliers, P. M., Collins, G. W., Da Silva, L. B., Gold, D. M., & Cauble, R. 1998, Appl. Phys. Lett., 73, 1320
Celliers, P. M., Collins, G. W., Da Silva, L. B., Gold, D. M., Cauble, R., Wallace, R. J., & Foord, M. E. 2000, Phys. Rev. Lett., in press
Chabrier, G., & Baraffe, I. 1997, A&A, 327, 1039
Chabrier, G., Saumon, D., Hubbard, W. B., & Lunine, J. I. 1992, ApJ, 391, 817
Collins, G. W., et al. 1998, Science, 281, 1178
———. 2000, Phys. Rev. Lett., submitted
Da Silva, L. B., et al. 1997, Phys. Rev. Lett., 78, 483
Evans, A. M., Freeman, N., Grahm, P., Horsfield, C., Rothman, S., Thomas, B., & Tyrrell, A. 1996, Laser Part. Beams, 14, 113
Gupta, Y. M., & Sharma, S. M. 1997, Science, 277, 909
Hemley, R. J., & Ashcroft, N. W. 1998, Phys. Today, 51(8), 26
Hemley, R. J., Mao, H. K., Goncharov, A. F., Hanfland, M., & Struzkin, V. 1996, Phys. Rev. Lett., 76, 1748
Holmes, N. C., Ross, M., & Nellis, W. J. 1995, Phys. Rev. B, 52, 15835
Hubbard, W. B. 1981, Science, 214, 145
Hubbard, W. B., Guillot, T., Lunine, J. I., Burrows, A., Saumon, D., Marley, M. S., & Freedman, R. S. 1997, Phys. Plasmas, 4, 2011
Kerley, G. I. 1972, Los Alamos Lab. Rep. LA-4776
Kerley, G. I. 1980, J. Chem. Phys., 73, 460
Koenig, M., et al. 1995, Phys. Rev. Lett., 74, 2260
Lenosky, T. J., Kress, J. D., & Collins, L. A. 1997, Phys. Rev. B, 56, 5164
Löwer, T., et al. 1994, Phys. Rev. Lett., 72, 3186
Loubeyre, P., LeToullec, R., Hausermann, D., Hanfland, M., Hemley, R. J., Mao, H. K., & Finger, L. W. 1996, Nature, 383, 702
Magro, W. R., Ceperley, D. M., Pierleoni, C., & Bernu, B. 1996, Phys. Rev. Lett., 76, 1240
Militzer, B., Magro, W. R., & Ceperley, D. M. 1998, in Strongly Coupled Coulomb Systems, ed. G. J. Kalman, K. B. Blagoev, & J. M. Rommel (New York: Plenum Press)
Narayana, C., Luo, H., Orloff, J., & Ruoff, A. L. 1998, Nature, 393, 46
Natoli, V., Martin, R. M., & Ceperley, D. M. 1993, Phys. Rev. Lett., 70, 1952
Nellis, W. J., Mitchell, A. C., van Thiel, M., Devine, G. J., & Trainor, R. J. 1983, J. Chem. Phys., 769, 1480
Nellis, W. J., Ross, M., & Holmes, N. C. 1995, Science, 269, 1249
Ng, A., Parfeniuk, D., & Da Silva, L. B. 1985, Phys. Rev. Lett., 54, 2604
Reinholz, H., Redmer, R., & Nagel, S. 1995, Phys. Rev. E, 52, 5368
Rogers, F. J. 1986, ApJ, 310, 723
Rogers, F. J., Swenson, F. J., & Iglesias, C. A. 1996, ApJ, 456, 902
Ross, M. 1998, Phys. Rev. B, 58, 669
Ross, M., Ree, F. H., & Young, D. A. 1983, J. Chem. Phys., 79, 1487
Saumon, D., & Chabrier, G. 1989, Phys. Rev. Lett., 62, 2397

Saumon, D., & Chabrier, G. 1991, Phys. Rev. A, 44, 5122
———. 1992, Phys. Rev. A, 46, 2084
Saumon, D., Chabrier, G., & Van Horn, H. M. 1995, ApJS, 99, 713
Saumon, D., Hubbard, W. B., Chabrier, G., & Van Horn, H. M. 1992, ApJ, 391, 827
Smoluchowski, R. 1967, Nature, 215, 691
Van Horn, H. M. 1991, Science, 252, 384
van Kessel, C. G. M., & Sigel, R. 1974, Phys. Rev. Lett., 33, 1020
Weir, S. T., Mitchell, A. C., & Nellis, W. J. 1996, Phys. Rev. Lett., 76, 1860
Wigner, E., & Huntington, H. B. 1935, J. Chem. Phys., 3, 764
Zeldovich, Y. B., & Raizer, Y. P. 1966, Physics of Shock Waves and High-Temperature Hydrodynamic Phenomena (New York: Academic)